SURFACE WAVE BEHAVIOR IN PHASED ARRAYS

FIRST QUARTERLY PROGRESS REPORT
28 OCTOBER 1965

SYLVANIA ELECTRONIC SYSTEMS
Government Systems Management
for GENERAL TELEPHONE & ELECTRONICS

FIRST QUARTERLY PROGRESS REPORT
ON
SURFACE WAVE BEHAVIOR IN PHASED ARRAYS

28 October 1965

Contract: AF 30(602)-3886
A.R.P.A. Order: #723

by

SYLVANIA ELECTRONIC SYSTEMS-EAST

SYLVANIA ELECTRONIC SYSTEMS
A Division of Sylvania Electric Products Inc.
100 First Avenue, Waltham, Mass. 02154

SUMMARY

Mutual coupling in phased arrays causes their active impedance to vary with the electrical phasing used to scan the array. Large impedance mismatches can accrue if many coupling contributions add in-phase. This happens when the steering phase advance equals the mutual coupling phase delay between consecutive elements. For these critical scan directions, reflections can be very large and the antenna array will transmit or receive very little power as evidenced by deep holes in the element radiation pattern. Element radiation pattern and active array mismatch are shown to be equivalent representations of phased array scanning performance.

A large, flat, uniformly spaced, array of identical elements is analyzed. A relation is found between the critical scan angle and mutual coupling coefficients. Radiation pattern and coupling phase measurements in an array are presented in support of the analysis.

This is the first quarterly technical report by Sylvania on contract AF 30(602)-3886 under Advanced Research Projects Agency order #723.

TABLE OF CONTENTS

LIST OF ILLUSTRATIONS

I Introduction:

Scan performance of large, phased array radars can be strongly effected by cumulative coupling between antenna elements in the array. Near certain critical scan directions, the radar steering phase advances approximately match the mutual coupling delays, thus many coupling contributions can accumulate in-phase to produce large active impedance mismatch and deep holes in the radar scan coverage.

This study is aimed at finding causes, consequences, and mechanisms for control of cumulative coupling (or Surface Waves) through:

1) analysis of large, planar, phased arrays
2) testing of various forms of the coaxial horn antenna in sample arrays
3) discussion with other laboratories who have critically tested or analyzed other types of antenna elements in phased arrays.

II Theory of Cumulative Coupling:

The character of cumulative coupling can be seen by analyzing the active reflection coefficient of an antenna element in a flat array.

The analysis here will be general; not unique to any particular antenna type. We will assume that the array is large, flat, and with uniform interelement spacing.

Figure 1 shows a linear sample from the interior of a uniform array. The array is driven by a sine wave source thru a power distribution and isolation network. All antenna elements are identical and spaced an equal distance "d_x". Currents on each antenna are all identical except for a ramp phase delay "ϕ" used to steer the array.

Transmission lines are shown connecting each antenna. Arrows show the intensity and phase of waves traveling toward and back from each antenna. This ratio of forward to backward wave is defined as the active reflection coefficient "Γ_a". It is independent of element position (neglecting end effects), but depends strongly on scan angle and electrical spacing between elements.

The active reflection coefficient at the array element "o" is the linear summation of the products of incident waves on each transmission line "E_m" times the mutual coupling coefficients "S_{om}" between the m^{th} and the o^{th} element.

$$\Gamma_a = \sum_m S_{om} \left(\frac{E_m}{E_o} \right) \qquad (1)$$

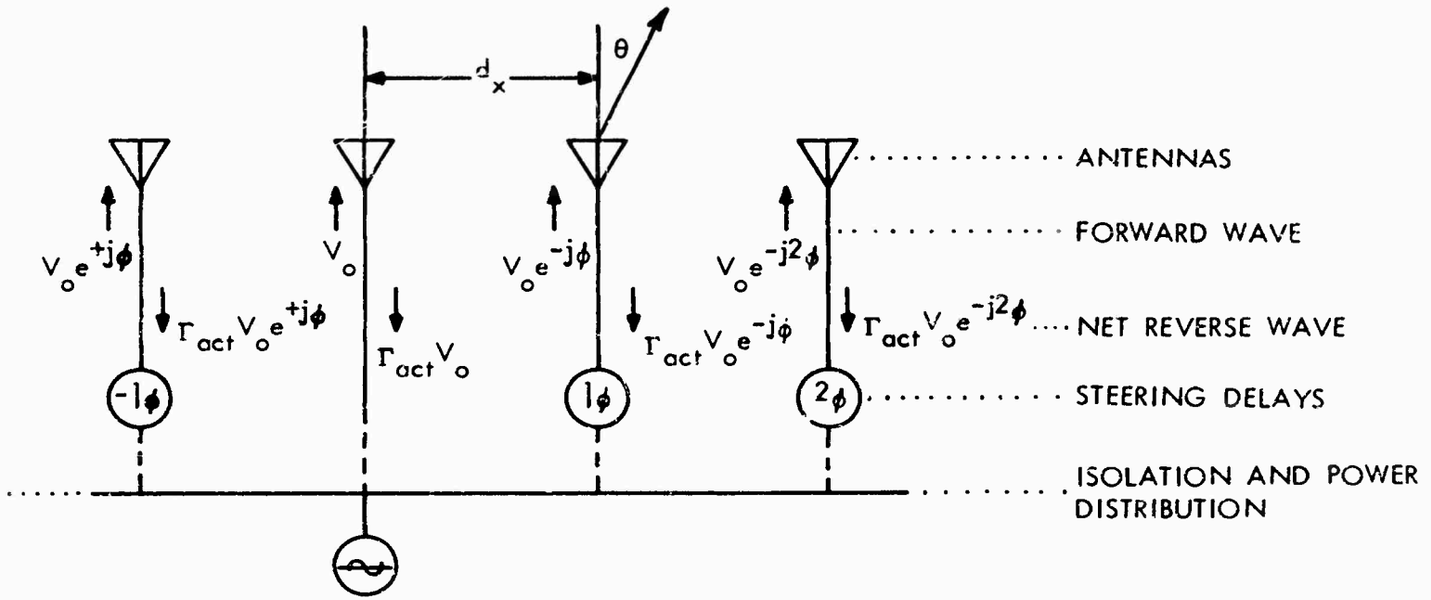

Figure 1. Traveling Waves on a Linear Array

(This exact equation can be regarded as the normalized o^{th} row of the usual scattering matrix representing the antenna array.) Equation (1) applys to either linear or planar arrays. In a linear array, the element is a single antenna. In a planar array each column (perpendicular to the plane of scan) has a common drive "E_m". "S_{om}" is then the coupling coefficient between that driven column "m" and the reference element "o". The summation is over the "m" columns in the array. Consecutive array columns are driven with the same amplitude and a uniform phase increment "ϕ" which steers the array radiation in the direction "θ_s". Tne phase increment "ϕ" and scan angle "θ_s" are related as follows:

$$\sin \theta_s = \frac{\lambda_c \phi}{2\pi d} \tag{2}$$

where:

$$\phi = \arg.\left(\frac{E_m}{E_{m-1}}\right) \tag{3}$$

Consecutive coupling coefficients "S_{om}" also have a nearly uniform phase progression as we will see later in Appendix B:

$$\psi \equiv \pm \text{ argument}\left(\frac{S_{o,m}}{S_{o,m-1}}\right) = d\,K_s = \frac{2\pi d}{\lambda_s} = \frac{wd}{v_s} \tag{4}$$

This last equation is a statement that the coupling phase delays vary linearly with the spacing between coupled elements. Effective wave number, wavelength, and phase velocity are defined in terms of these measurable coupling phase delays at the discrete antenna terminals.

We now have expressions for the two factors "E_m" and "S_{om}" producing the active mismatch. Combining the first 4 equations yields the 5^{th}:

$$\Gamma_a = S_{oo} + \sum_{m>o} \left| \frac{E_m}{E_o} S_{om} \right| \left\{ e^{jm(\psi-\phi)} + e^{jm(\psi+\phi)} \right\} \tag{5}$$

The array active reflection coefficient is seen to be the sum of coupling contributions from the central column and from columns on either side. These coupling effects can accumulate in-phase and yield large array mismatches. When the steering advance "ϕ" equals the coupling delay "ψ" plus any multiple of 2π, then at least one of the exponents is zero and many coupling terms add in-phase. This scan condition, when consecutive array columns couple in-phase, will be called the critical scan angle and will be evaluated via equations 2 & 4.

Equation 6 shows how the critical scan angle depends on array spacing "d" and on coupling phase velocity "v_s":

$$\sin \theta_{sc} = \pm\left(\frac{\lambda_o}{d} - \frac{c}{v_s}\right) \qquad (6)$$

The critical scan direction is the difference between the inverse electrical spacing and the inverse relative coupling velocity. Equation 7 gives the scan angle which produces a grating lobe maxima along the ground plane:

$$\sin \theta_{sg} = \frac{\lambda_o}{d} - 1 \qquad (7)$$

We can compare these two scan angles, and see that if the coupling velocity "v_s" is less than the velocity of light (this is the usual case), then the critical scan angle "θ_{sc}" yielding maximum impedance mismatch is smaller than the scan angle "θ_{sg}" yielding an end-fire grating lobe. Consequently, a phased array whose design is based entirely on grating lobe consideration , could show serious impedance and radiation defects within its design coverage.

III Arrays Under Test:

To check the above theory, sample hexagonal arrays were constructed and are undergoing extensive electrical measurement. The antenna elements are coaxial horns as shown in figure 2. Each antenna consists of a pair of concentric cylinders propagating the TE_{11} coaxial mode, shown in the top view of the antenna. This mode is launched by a radial probe $\frac{\lambda}{4}$ from the bottom of the antenna cavity and travels upward thru a quarter-wave-plate, radiating circular polarization. (The quarter-wave plate will be removed shortly and tests will continue on the linearly polarized antenna array. All tests reported here are on circular polarized antenna elements.)

These coaxial horn antennas were assembled in several different planar arrays, each having hexagonal-interelement geometry. Figure 3 shows the smallest array containing 52 antenna elements. The largest array* was a circular disk containing over 2,000 elements. Similiar element performance was obtained in each array. Element radiation pattern and interelement complex coupling coefficients were measured and correlated.

Appendix A shows that element radiation pattern and active array mismatch are equivalent. Consequently, scan performance of large, planar, phased arrays can be

*The 2000 element Mar receiver array was developed by Sylvania for Bell Telephone Labs. under contract DA-30-069-ORD-1955. Coupling measurements were funded under that contract. Technical results are reported here because of their relevance to this surface wave study.

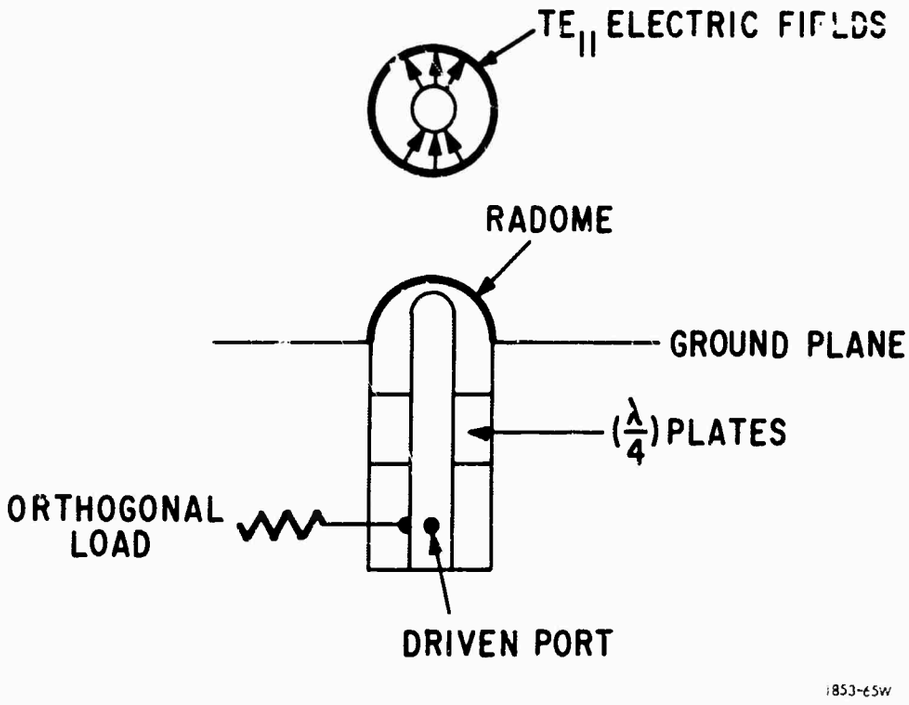

Figure 2. Antenna Cross Section

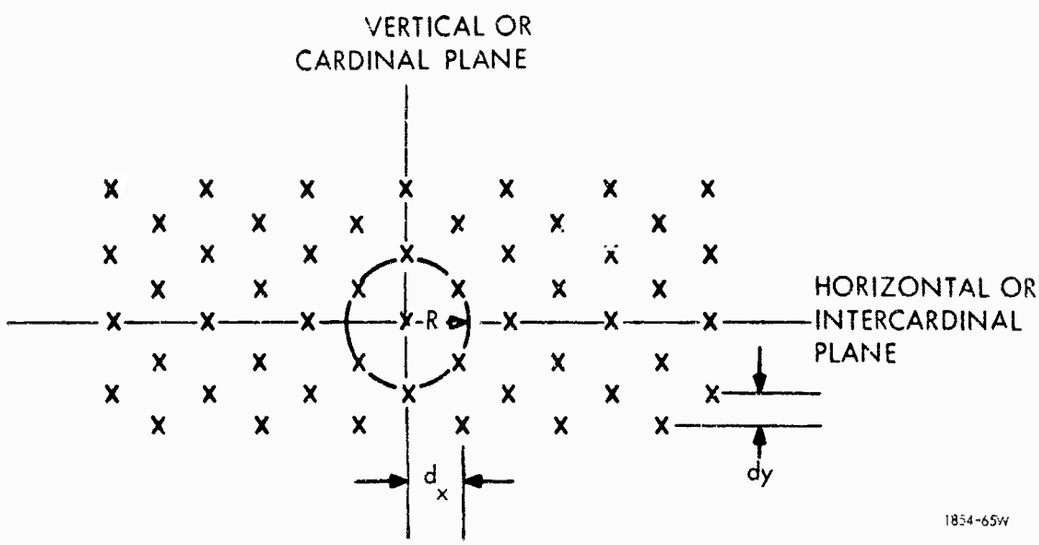

Figure 3. 52 Element Array

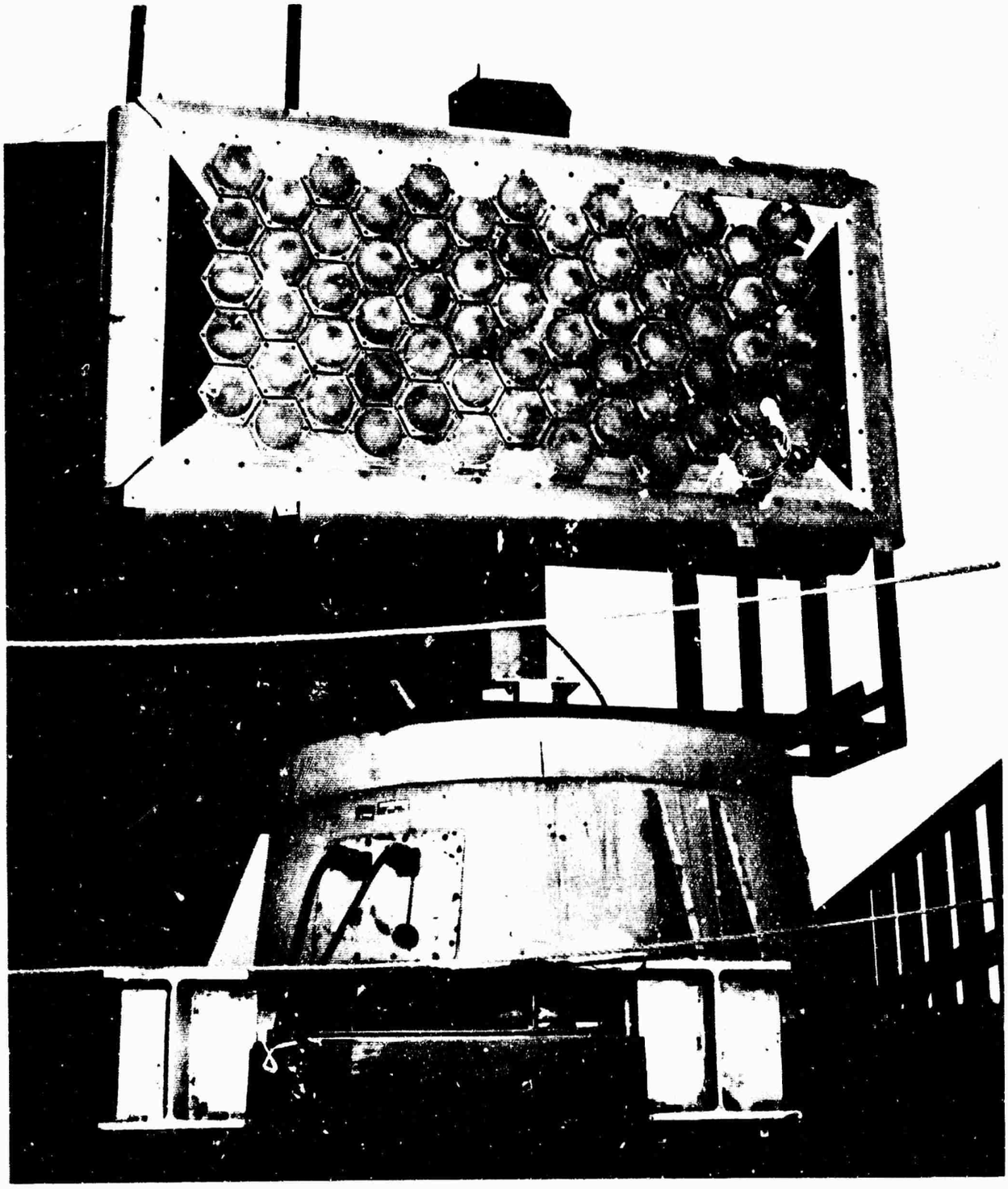

Figure 3A. 65-Element Array

evaluated by measurement of either element radiation pattern or active array mismatch. Measurement of element radiation pattern is, by far, the simpler technique and will be described next.

IV Radiation Pattern Measurements:

Element radiation patterns were measured by connecting one central antenna element to a receiver and passively terminating all neighboring elements in the test array. The array was mounted on a recorder turntable with the aperture of the central element near the axis of rotation. A 4 foot paraboloidal transmitter dish was located about 40 feet away. The transmitter feed dipole rotated to sample array response to electric field polarizations:

1. in the plane of scan (horizontal polarization)
2. perpendicular to the plane of scan (vertical polarization) and
3. rapidly spinning to show polarization ellipticity.

Test variables have included: 6 microwave frequencies, 3 transmitter polarizations, 3 load impedances, and 2 planes of scan.

Figures 4, 5, and 6 are samples of element radiation patterns measured in the horizontal plane of a 52 element array. Figure 4 shows antenna element response to an electric field component in the plane of scan; figure 5 shows the response to an electric field component perpendicular to the plane of scan; and figure 6 shows the polarization ellipticity and power density vs angle. For all 3 radiation patterns, scanning was in an intercardinal plane (fig. 3), angles were measured from array broadside, and electrical spacing was: $d_x = 0.506\ \lambda_o$.

Under these conditions, grating lobe maxima remain outside real space for all scan angles up to $\pm 78^\circ$; yet deep holes at 65° are seen in the element pattern (fig. 4). The antenna element had been previously tested as a single element on a large ground plane. The isolated element pattern showed good coverage with no radiation holes. When placed in an array of like elements, nulls appeared as shown here. These nulls are a consequence of mismatch thru in-phase coupling accumulation. Note also, that the nulls appear only in figure 4, where the electric field is in the plane of scan and hence couples strongly and in-phase, to many neighboring elements. The electric field component, perpendicular to the plane of scan, is tangential to the array face and does not propagate along the array face, consequently no nulls appear in figure 5.

In figure 4, the depth and angular position of the radiation nulls depend on the impedance terminating the passive array elements. This seems to be a consequence of a reactive component of perodic loading presented, by the antenna elements, to the mutual coupling wave traveling across the array face. Reactive loading of a transmission line is known to influence phase velocity; a similiar effect could occur here. Equation (6) showed that a

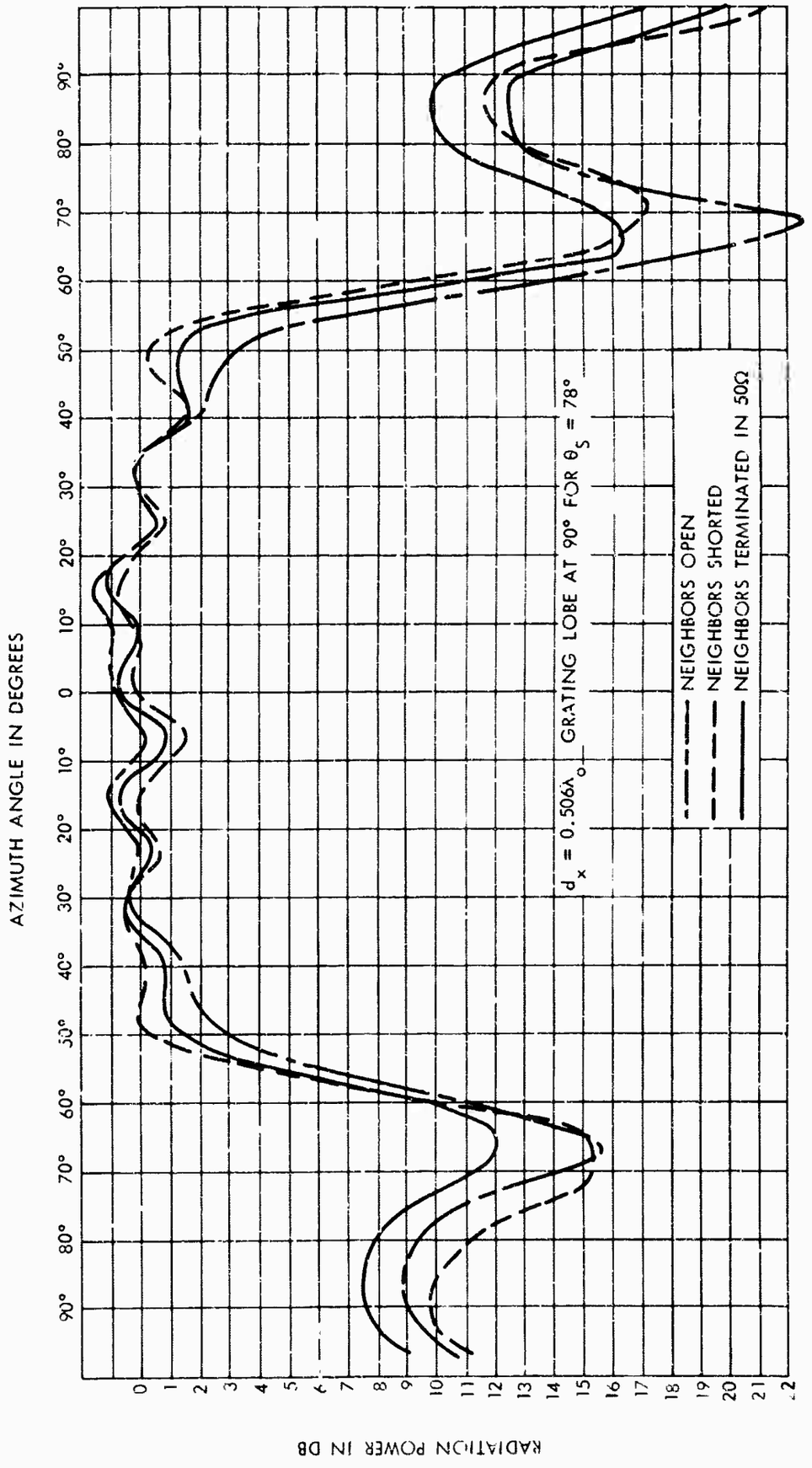

Figure 4. Horizontal Polariz[illegible]n, Horizontal Scan Cut

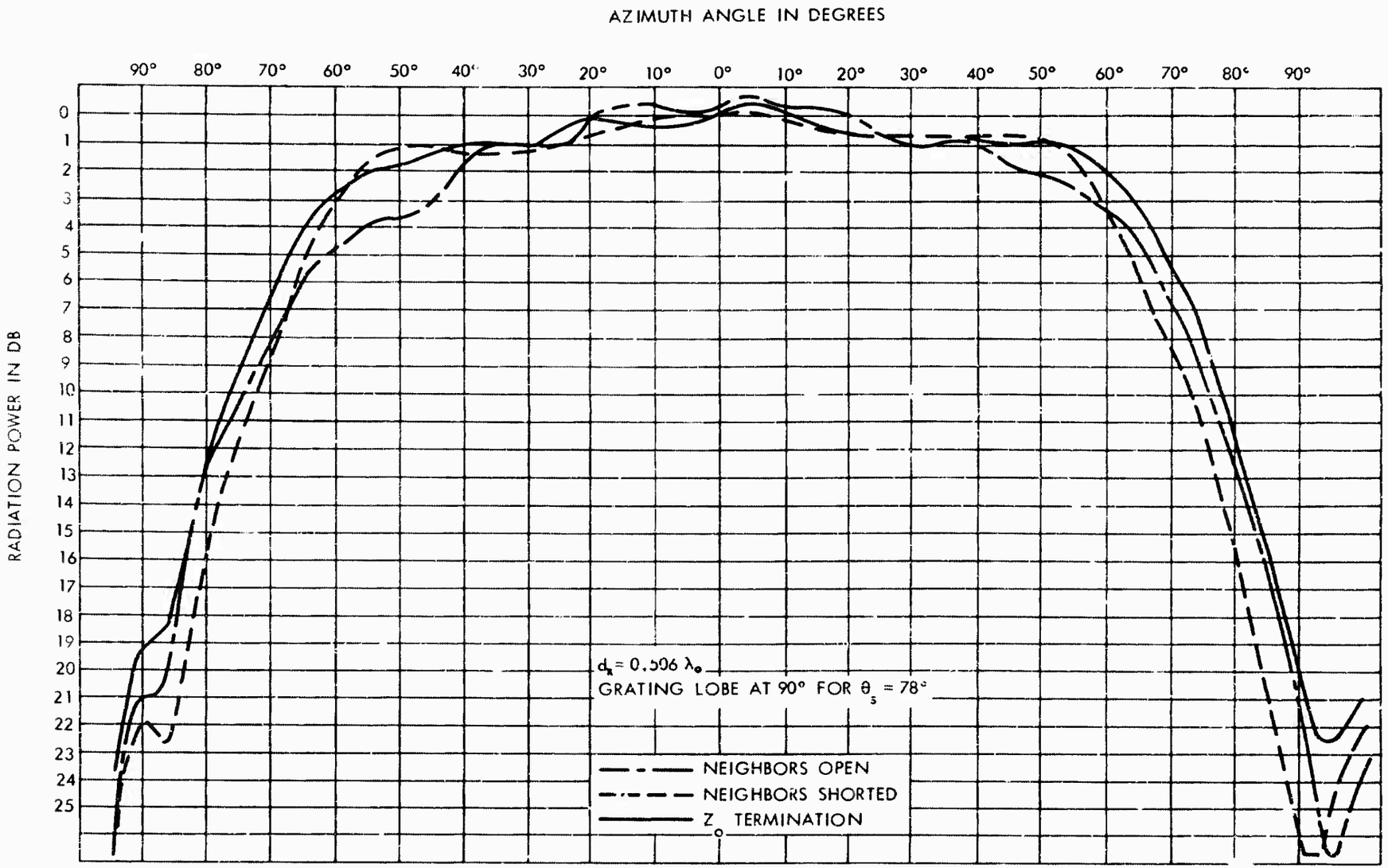

Figure 5. Vertical Polarization, Horizontal Scan Cut

1852-65W

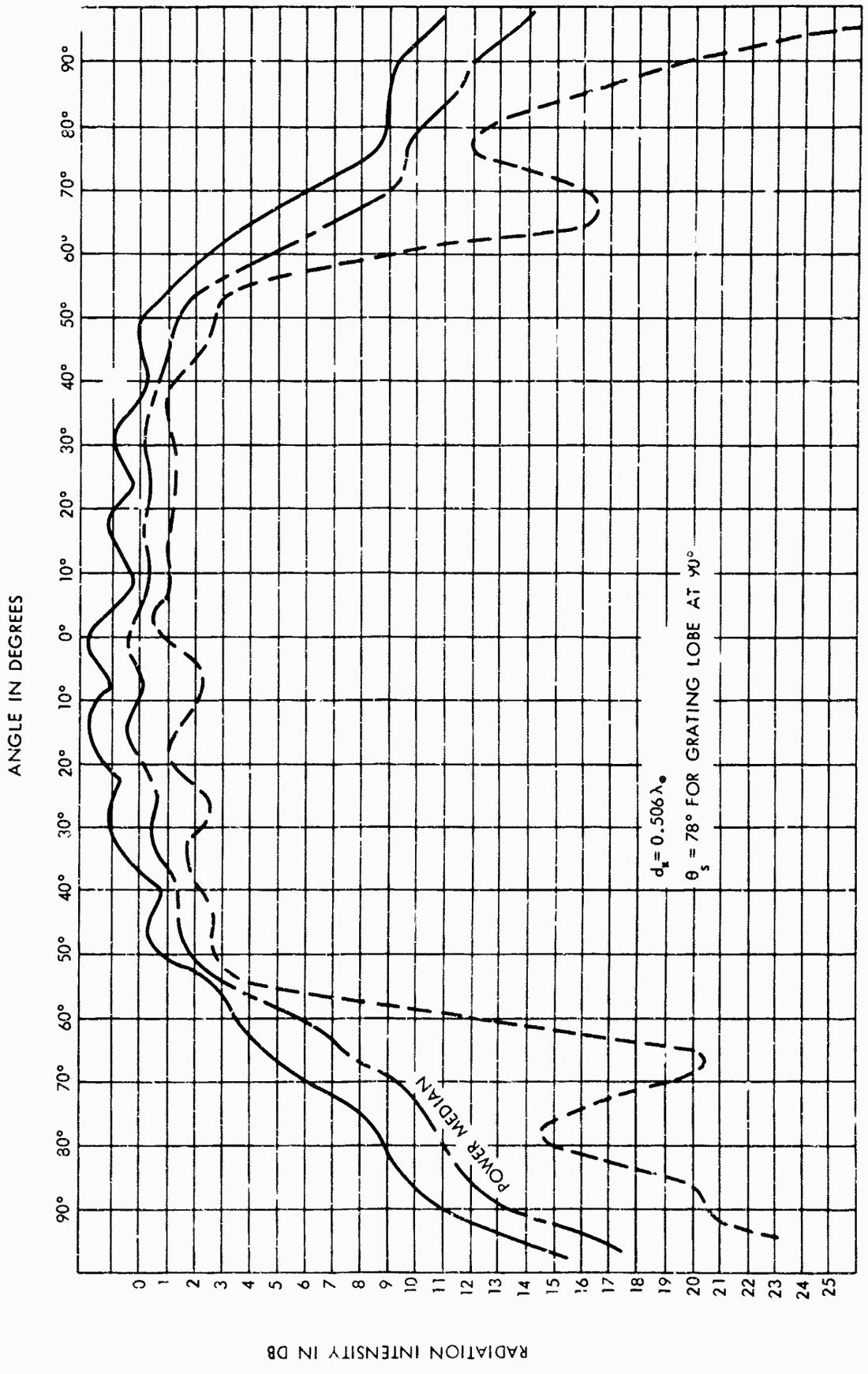

Figure 6. Rotating Linear Polarization: Ellipticity Envelope and Angular Distribution of Net Radiant Power Density. Horizontal Scan Cut

change in the velocity of the coupling wave changes the angular position of the radiation nulls. The effect of terminal impedance on phase velocity and null position is slight suggesting that individual coaxial horns couple weakly to the "surface wave".

In the analysis presented in section II, we found that the critical scan angle could be determined from measurements of either element radiation pattern intensity or the phase of the coupling coefficients (Appendix B). Both tests have been made, at many different radio frequencies. These test results have been correlated in figure 7. Abscissa is the electrical spacing between elements, projected on the plane of scan. The ordinate is the angle from broadside at which the radiation null appeared or was predicted. Frequency is the independent variable in this experiment. The "x" in the graph represent measured radiation nulls for scanning in the intercardinal plane. "o" represent independent measurement of coupling phase. Radiation intensity and coupling phase measurements agree very well with theory for the closer electrical spacings and smaller scan angles. At higher frequencies, two nulls are sometimes observed. In every case, the null nearest broadside is predicted accurately by this cumulative coupling theory. The second null at a wider scan angle implies radiation of power thru a grating lobe in real space. The curve shows those combinations of scan angle and electrical spacing for which the grating lobe peak is just end-fire (parallel to the array face). Note that throughout these tests, the critical scan angle yielding large impedance mismatch is about 10° smaller than the scan angle producing a real grating lobe. Scan performance of this array is therefore limited, not by classical grating lobe considerations, but rather by the cumulative coupling effect.

Figure 4, 5, and 6 show measured element radiation patterns in an intercardinal plane of the array (i.e. horizontal in figure 3). Because of hexagonal array symmetry, the element radiation pattern should repeat in each of the 6 principal intercardinal planes of scan spaced at 60° increments of longitude. In each of these planes, projected interelement spacing is large $d_x = 0.886R$, hence, grating lobe and cumulative coupling effects can occur inside real space.

In contrast, the 6 cardinal planes have close interelement spacing $d_y = 0.500R$. Consequently grating lobe and cumulative coupling effects occur at wider scan angles (generally outside real space). This theory was checked by measuring elevation pattern of the array similar to figure 3. Tests were made at several different frequencies and using the 3 previous test polarizations. No symmetric cumulative coupling nulls were found. Figure 8 shows a typical, cardinal plane pattern. The intercardinal plane cut (figure 4) shows nulls; the cardinal plane (figure 8) does not. Figure 9 is an estimate of three dimensional scan performance. The array is in the X-Y plane; scan coordinates are the direction cosines to these principal axis. The large circle represents the limit of steering along the plane of the array: $\cos^2(\alpha_x) + \cos^2(\beta_y) = 1$. The 6 sided scallop is a possible contour of maximum cumulative coupling. It extends inside real space in the 6 intercardinal directions and is outside real scan space in the 6 cardinal directions as suggested by the horizontal and vertical radiation pattern cuts in figure 4 and 8 respectively.

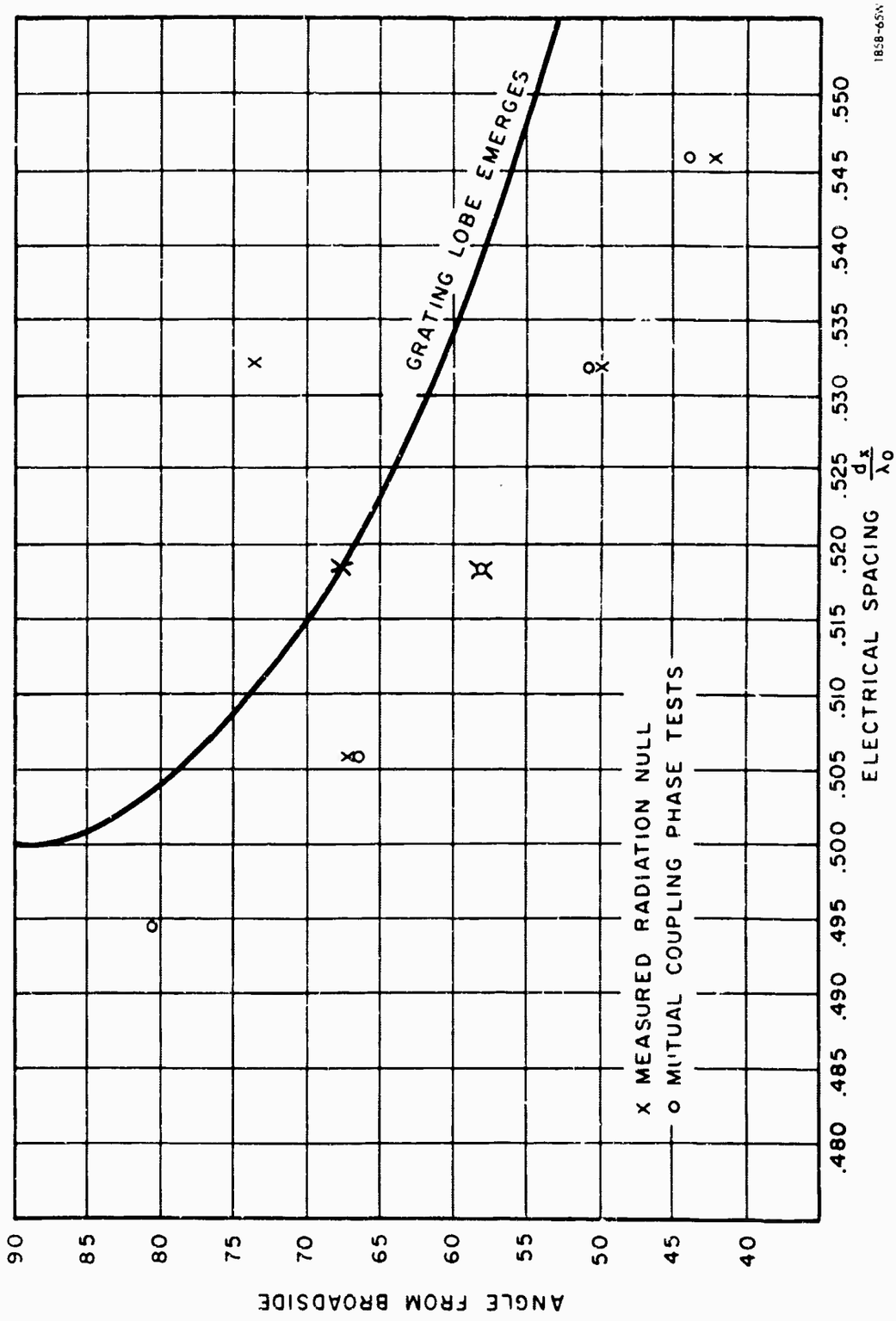

Figure 7. Scan Angle Yielding Radiation Nulls

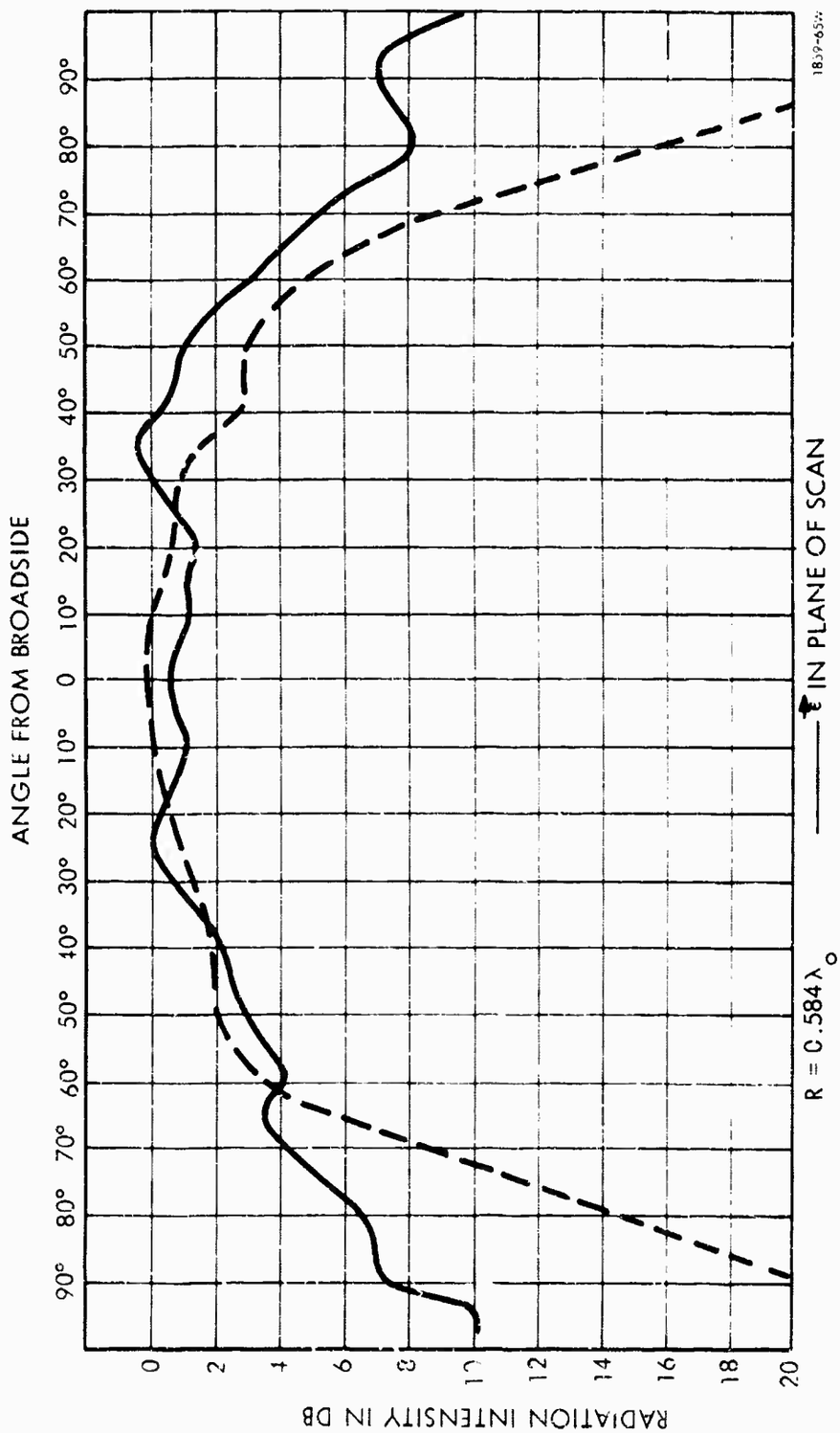

Figure 8. Element Radiation Pattern, Cardinal Plane

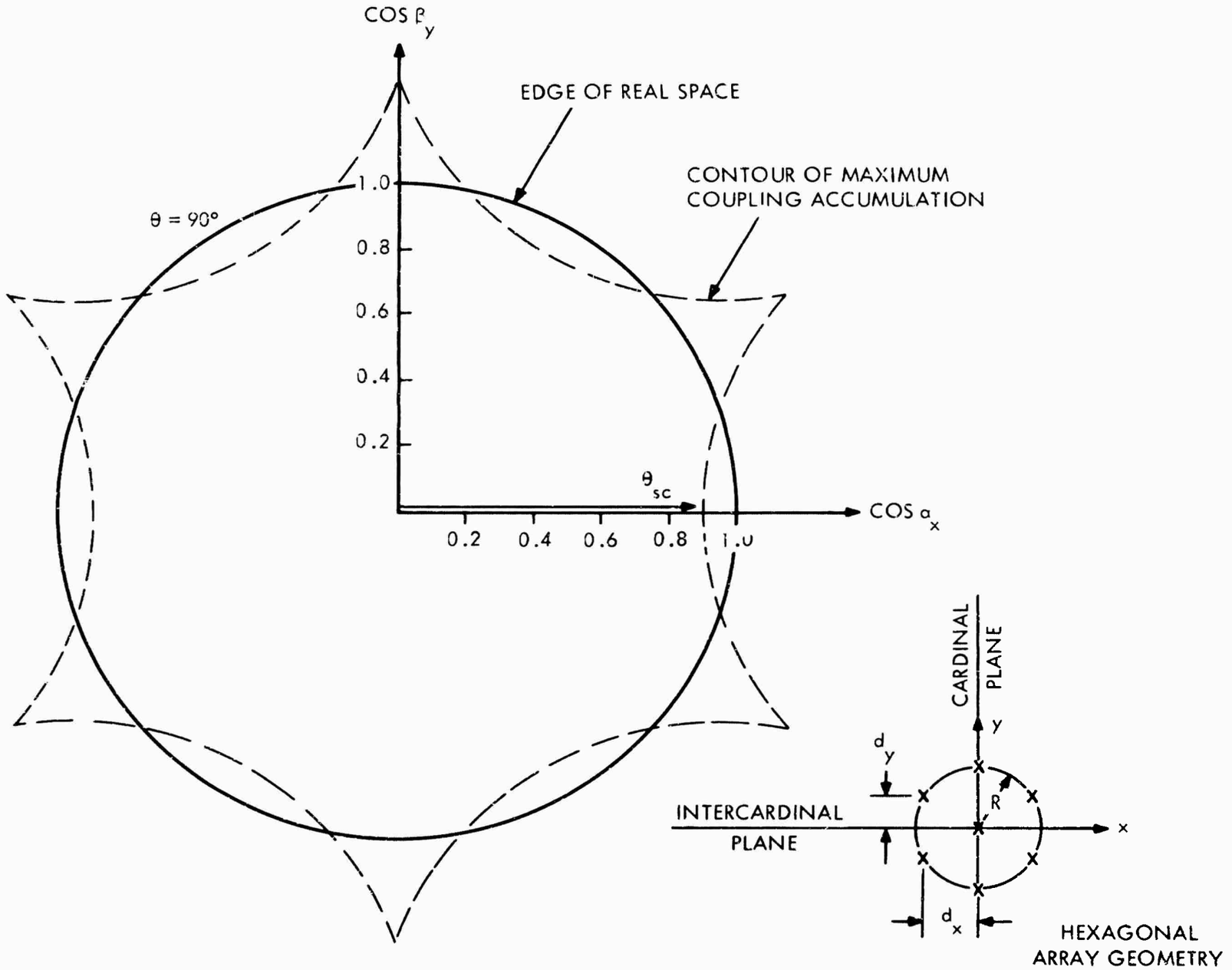

Figure 9. Critical Scan Directions

V Presentations & Publications:

A) "Cumulative Coupling in Antenna Arrays" by L. W. Lechtreck presented at the International Antenna & Propagation Symposium on Aug. 31, 1965.

B) "Scan Relationships in Planar Phased Arrays" by L. W. Lechtreck in preparation.

APPENDIX A

SCAN RELATIONSHIPS IN PLANAR PHASED ARRAYS

by L. W. Lechtreck

INTRODUCTION

Large, planar, phased arrays can be electronically scanned by suitably controlling the phase of radiation from each antenna element. The required phasing of each antenna is uniquely determined by the desired scan direction ($\theta_s \phi_s$) and by the element location in the array. (A planar aperture phase front is assumed.)

Radiation performance of a planar array is a function of scan angle and usually deteriorates sharply as the scan angle "θ_s" approaches 90°. The exact character of this scan degradation depends on the design of the antenna element and on array geometry. However, for any given array design, there exist certain fixed relationships between the scan variables, specifically:

1) radiation power density on a target,

2) element radiation pattern,

3) array efficiency,

4) active impedance mismatch, and

5) solid angle spanned by the radiation beam.

This paper will derive equations relating these phased array scan variables.

The derivation is based on equating the power delivered by the feed lines to the power radiated by the array. It is complicated by the fact that different elements in the array can have differing radiation and impedance characteristics because of: antenna element variations, space taper, or edge effects. To include these effects, we will define: a mean active reflection coefficient, a mean element radiation pattern, and an effective radiation solid angle.

CO-ORDINATES

Before proceeding with the derivation, it is necessary to define a co-ordinate system and certain electrical symbols. A large planar array of antenna elements is sketched below.

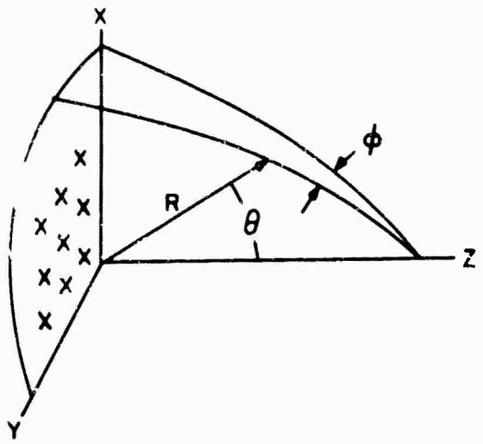

The array face is the "x-y" plane; its normal is the "z" axis. Spherical angle "θ" is measured from the array normal and "ϕ" is the longitude about the Z axis (pole of the spherical co-ordinates). Subscript "s" refers to the steering commands, and "m" are indices identifying the antenna element having co-ordinates "x_m, y_m".

To electrically steer the array in the direction $\theta_s\phi_s$, the m^{th} element will be phased[1]:

$$\psi_m = \left(\frac{2\pi}{\lambda_o}\right) \sin\theta_s \left[x_m \cos\phi_s + Y_m \sin\phi_s\right] \qquad (1)$$

Define the following symbols:

V_m = incident voltage driving the m^{th} antenna element

$E_m(\theta o)$ = electric field radiated by the m^{th} element per unit incident voltage, rest terminated in Z_o

$\Gamma_m(\theta_s\phi_s)$ = active reflection coefficient at m^{th} element

Z_o = characteristic impedance of th transmission lines

No = characteristic impedance of free space = 377 ohms

$\eta_a(\theta_s\phi_s)$ = array efficiency = $\frac{\text{power radiated by the a ay}}{\text{power consumed by the array}}$

$P(\theta_s\phi_s)$ = total power (watts) radiated by the array

θ, ϕ = spherical radiation angles

(θ_s, ϕ_s) = array steering direction

E_Σ = radiated field intensity (volts/meter), by linear superposition of contributions from each antenna element

DELIVERED POWER

The total power available from a phased array is independent of scan:

$$\sum_m \frac{|V_m|^2}{2Z_o}$$

Total power delivered depends on scan direction:

$$p(\theta_s\phi_s) = \eta_a(\theta_s\phi_s)\sum_m \frac{|V_m|^2}{2Z_o}\left\{1 - |\Gamma_m(\theta_s\phi_s)|^2\right\} \tag{2}$$

$$p(\theta_s\phi_s) = \eta_a(\theta_s\phi_s)\left\{1 - |\bar{\Gamma}(\theta_s\phi_s)|^2\right\}\left(\frac{1}{2Z_o}\right)\sum_m |V_m|^2 \tag{3}$$

where a mean reflection coefficient is defined as:

$$1 - |\bar{\Gamma}(\theta_s\phi_s)|^2 = \frac{\sum_m \left[|V_m|^2\left\{1 - |\Gamma_m(\theta_s\phi_s)|^2\right\}\right]}{\sum_m |V_m|^2} \tag{4}$$

If the active reflection coefficient is the same throughout the array, then that is also the value of the mean reflection coefficient. Otherwise, it is the weighted average given in equation (4).

TOTAL POWER RADIATED

A radar target is illuminated by an incident electric field intensity which is the linear superposition of contributions from each antenna element in the transmitter array. The resulting summation is a function of the angular location of the target ($\theta\phi$) and of the direction of array electrical scan ($\theta_s\phi_s$). We assume that the radar beam is steered to the direction of the target so that $\theta = \theta_s$ and $\phi = \phi_s$.

$$E_\Sigma\begin{pmatrix}\theta=\theta_s\\ \phi=\phi_s\end{pmatrix} = \sum_m |V_m| E_m(\theta_s\phi_s) = \bar{E}(\theta_s\phi_s)\sum_m |V_m| \tag{5}$$

where the mean element pattern has been defined as:

$$\bar{E}(\theta_s\phi_s) = \frac{\sum_m |V_m| E_m(\theta_s\phi_s)}{\sum |V_m|} \tag{6}$$

If the element pattern is homogeneous throughout the array,[2] then the mean and homogeneous element patterns are the same. Otherwise the mean pattern is a weighted average given in equation (6). For radiation in the direction of scan ($\theta = \theta_s$, $\phi = \phi_s$), the radiation retardation and the steering phase advance "ψ_m" are exact compliments for every element in the array. These canceling phases are hence deleted from the drives $|V_m|$ and the element responses:

$E_m(\theta_s\phi_s)$ and $\bar{E}(\theta_s\phi_s)$ in equations (5) and (6).

Equation (5) shows that when a phased array is steered in the direction of a radar target $(\theta = \theta_s)(\phi = \phi_s)$, the target illumination

$$\left| \bar{E}_\Sigma \left(\begin{matrix} \theta=\theta_s \\ \phi=\phi_s \end{matrix} \right) \right|^2$$

is proportional to the mean element power pattern $|\bar{E}(\theta_s\phi_s)|^2$. (The factor $\left\{ \sum_m |V_m| \right\}^2$ is a constant for all scan directions.)

Total far field power radiated by a phased array is the integral of the power density over any sphere in the far field. The observer co-ordinates (θ, ϕ) are now integration variables; and steering angles $(\theta_s\phi_s)$ are held constant during integration.

$$P(\theta_s\phi_s) = \iint \frac{|E_\Sigma(\theta, \theta_s, \phi, \phi_s)|^2}{2N_o} \, da = \frac{R^2}{2N_o} \iint |E_\Sigma(\theta\theta_s\phi\phi_s)|^2 d\Omega \tag{7}$$

Next define an effective solid angle "$\bar{\Omega}_i$" surrounding each major radiation lobe in real space:

$$\bar{\Omega}_i = \frac{\int\int |E_{\Sigma i}(\theta\theta_s\phi\phi_s)|^2 d\Omega}{\left| E_{\Sigma i} \left(\begin{matrix} \theta=\theta_s \\ \phi=\theta_s \end{matrix} \right) \right|^2} = \frac{\int\int |E_{\Sigma i}(\theta_s\theta\phi_s\phi)|^2 d\Omega}{|\bar{E}_i(\theta\phi)|^2 \left\{ \sum_m |V_m| \right\}^2} \tag{8}$$

Combining equations (7) and (8) yields an expression for net power radiated by the array in terms of the effective solid angle surrounding each major beam (main lobe and grating lobes):

$$P(\theta_s\phi_s) = \frac{R^2 \left\{ \sum_m |V_m| \right\}^2}{2N_o} \sum_{\substack{ML \\ GL}} |\bar{E}(\theta_i\phi_i)|^2 \bar{\Omega}_i \tag{9}$$

POWER CONSERVATION

Equating the net radiated power (9) with the net power delivered by the array (3) yields:

$$\sum_{\substack{ML\\GL}} |\bar{E}_i(\theta_i\phi_i)|^2\,\bar{\Omega}_i = \left[\frac{N_o}{Z_o R^2} \times \frac{\sum_m |V_m|^2}{\left\{\sum_m |V_m|\right\}^2}\right] \times \eta_a(\theta_s\phi_s)\left\{1 - |\bar{\Gamma}(\theta_s\phi_s)|^2\right\}$$

The factor in square brackets on the right is a constant "C_o" for any radar range and radar system design. The remaining scan dependence is:

$$\sum_{\substack{M.L.\\G.L.}} |E_i(\theta_i\phi_i)|^2\,\bar{\Omega}_i = C_o\eta_a(\theta_s\phi_s)\left\{1 - |\bar{\Gamma}(\theta_s\phi_s)|^2\right\} \tag{10}$$

If the phased array radiates only one major lobe in real space, then the left hand summation reduces to a single term describing that steered lobe:

$$|\bar{E}(\theta_s\phi_s)|^2\,\bar{\Omega}(\theta_s\phi_s) = C_o\eta_a(\theta_s\phi_s)\left\{1 - |\bar{\Gamma}(\theta_s\phi_s)|^2\right\} \tag{11}$$

SCANNING VARIATIONS

We can compare the radiation intensity in any two array steering directions $\theta_1\phi_1$ and $\theta_2\phi_2$:

$$\frac{\vec{P}(\theta_1\phi_1)}{\vec{P}(\theta_2\phi_2)} = \frac{|\bar{E}(\theta_1\phi_1)|^2}{|\bar{E}(\theta_2\phi_2)|^2} = \frac{\eta_a(\theta_1\phi_1)}{\eta_a(\theta_2\phi_2)} \times \frac{1 - |\bar{\Gamma}(\theta_1\phi_1)|^2}{1 - |\bar{\Gamma}(\theta_2\phi_2)|^2} \times \frac{\bar{\Omega}(\theta_2\phi_2)}{\bar{\Omega}(\theta_1\phi_1)} \tag{12}$$

Equation (12) shows that the target illumination and mean element radiation power pattern are each proportional to the array efficiency (dissipative and reflective) and inversely proportional to the effective radiation solid angle "$\bar{\Omega}$".

"$\bar{\Omega}$" can be computed from the net array radiation pattern via definition (8). For example, we can estimate the effective solid angle of a phased array radiating a single steerable pencil beam surrounded by sidelobes whose intensities either decay or have uniform maxima and cosine shape throughout the hemisphere in front of the array face.

$$\bar{\Omega}(\theta_s\phi_s) \approx \frac{K\,Bw^2(0)}{\cos\theta_s} + \left(\frac{\pi}{2}\right)\frac{\left|\bar{E}_\Sigma \text{ S. L. peaks}\right|^2}{\left|E_\Sigma\left(\substack{\theta=\theta_s\\\phi=\phi_s}\right)\right|^2} \tag{13}$$

The coefficient "K" depends on the specific radiation pattern shape K = 1.2 for the radiation pattern $E_{\Sigma} = \frac{J_1(u)}{u}$; K = 1.3 for the pattern $E_{\Sigma} = \frac{\sin x}{x} \times \frac{\sin y}{y}$. Cosine θ_s in the denominator is a consequence of main lobe broadening in the plane of scan and is valid for steering short of end-fire:

$$\theta_s < \frac{\pi}{2} - \sqrt{Bw(0)} .$$

The last term in equation (13) represents the net power radiated thru wide angle side lobes. It is the product of the normalized side lobe peak power, times the mean value of the side lobe power pattern $(\cos u)^2 (\cos v)^2 \rightarrow .25$, times the net solid angle containing these uniform side lobes (typically 2π steradians for side lobes spanning half space). For large thinned arrays with strong Tchebyscheff side lobes, the second term can dominate. For large arrays having weak and rapidly decaying side lobes, only the first term in (13) is used.

If the wide angle sidelobe energy is negligible and if the array is not steered close to end fire, then equations (12) and (13) combine to yield the following radar scan equation:

$$\frac{\vec{P}(\theta_1\phi_1)}{\vec{P}(\theta_2\phi_2)} = \frac{|\bar{E}(\theta_1\phi_1)|^2}{|\bar{E}(\theta_2\phi_2)|^2} = \frac{\eta_a(\theta_1\phi_1)}{\eta_a(\theta_2\phi_2)} \times \frac{1 - |\bar{\Gamma}(\theta_1\phi_1)|^2}{1 - |\bar{\Gamma}(\theta_2\phi_2)|^2} \times \frac{\cos\theta_1}{\cos\theta_2} \qquad (14)$$

Target illumination and element power pattern are each proportional to the dissipative and reflective efficiency of the array times the cosine of the scan angle. Constant array efficiency and match imply a cosine element power pattern as was pointed out in reference (4).

The intensity of radiation from a phased array radar decreases with increasing scan angle according to equation (14). The "cosineθ" factor is weakest for scanning near "end-fire". A planar array having a 1° circular beam at broadside, will have a 1° × 11° oval beam near "end-fire", which will contribute a two-way radar echo degradation exceeding 20 db. Further substantial losses can accrue from impedance mismatch,[5,6] usually worst when a major lobe approaches "end-fire".

SUMMARY

Equations have been derived relating several critical phased array performance figures: target illumination, antenna element pattern, array efficiency, impedance mismatch, and effective radiation solid angle. Each depends on the electrical scanning of the array $(\theta_s\phi_s)$. Element radiation pattern in a passive array and active mismatch in a phased array are seen to be equivalent representations of array scanning performance. Results apply to any large, planar, phased array with the observer in the direction of scan. Included is an upper bound on wide angle performance of planar, phased array systems when perfectly match and lossless.

BIBLIOGRAPHY

1. W. Von Aulock, "Properties of Phased Arrays", Proceedings of IRE, October 1960, pp. 1715-1727.

2. L. Lechtreck, "Green's Function in Space Tapered Arrays", IEEE Transactions on Antennas and Propagation, May 1964, pp. 366-367.

3. R.S. Elliott, "Beamwidth and Directivity of Large Scanning Arrays", The Microwave Journal, December 1963 and January 1964.

4. L. Parad, "Some Mutual Impedance Effects in Phased Array", The Microwave Journal, June 1962, pp. 87-89.

5. J. Allen, "Mutual Coupling---Why Worry About It", 1965 International Antenna & Propagation Symposium Program & Digest, pp 133-137.

6. L. Lechtreck, "Cumulative Coupling in Antenna Arrays", 1965 International Antenna & Propagation Symposium Program & Digest, pp. 144-149.

APPENDIX B

COUPLING COEFFICIENTS MEASUREMENTS

The active match of an element in a large phased array is determined entirely by the relative drives of its neighbors and by their coupling coefficients. Extensive coupling measurements were made in the central region of a 2000 element, hexagonal array of coaxial horn antennas. A transmitter was connected to the central element and a receiver connection was moved from one element to the next along the 6 principal radials in the array. All unused elements were terminated in 50 Ω resistors. Figure B-1 shows how the measured coupling phase depends on relative distance and direction between the coupled elements. The abscissa is the distance between coupled elements, normalized to the free space wavelength; the ordinate is measured phase normalized to 2π. Entries appear at the discrete distances corresponding to the centerlines of each consecutive antenna element. The three lines connect test points in the three cardinal directions in the hexagonal array. Two important facts are evident in this graph. First, the coupling phase varies linearly with distance. The slope of each curve shows the phase velocity in that direction. For this array, the phase velocity was 90 to 95% of the free space velocity of light. Coupling phase also depends on the relative direction of the coupled elements. The three lines on this graph are displaced vertically by 120°. Circular polarization theory predicts a 120° coupling phase change for each 60° increase in angle between coupled elements.

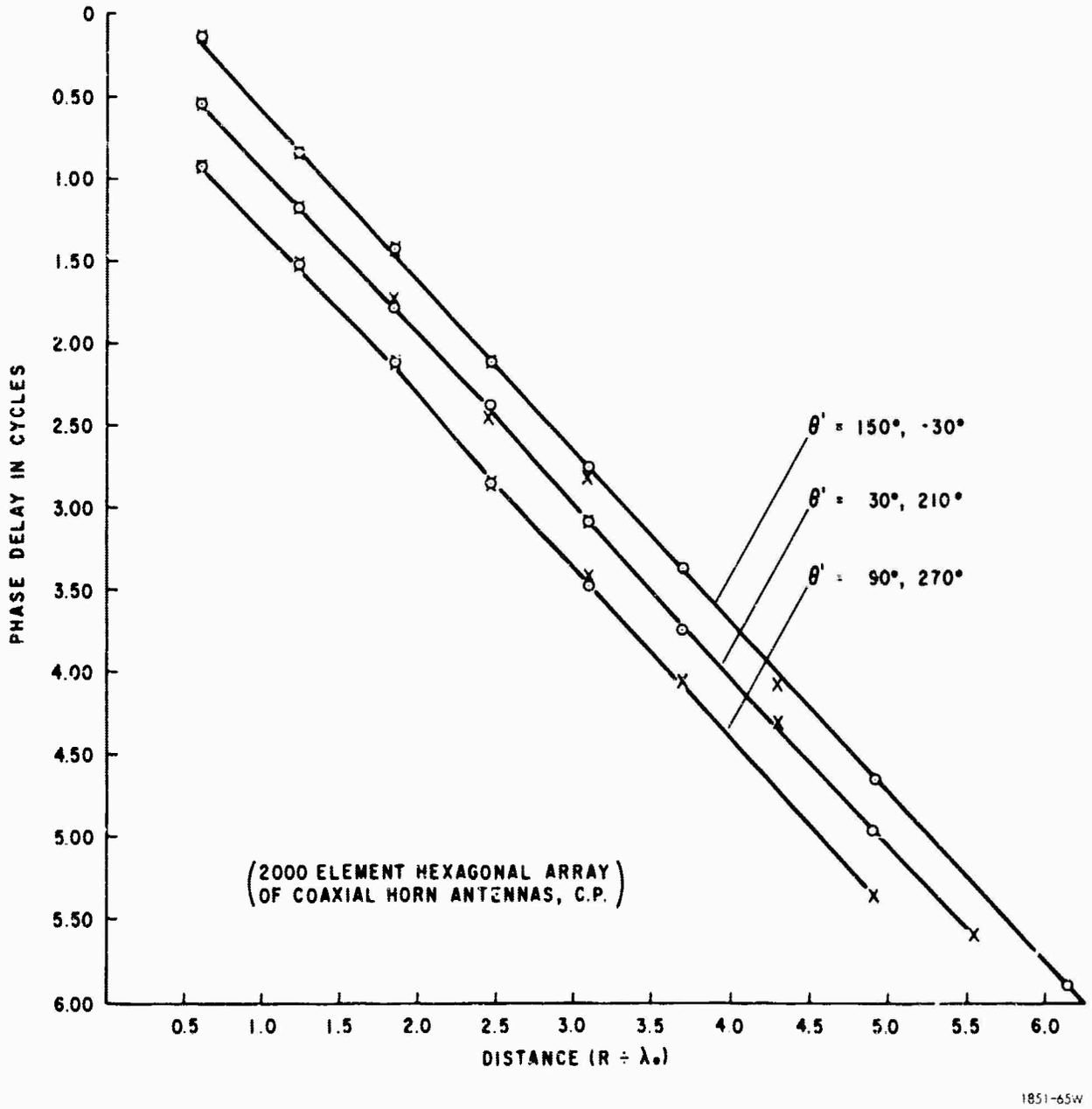

Figure B-1. Coupling Phase Measurements